RSC Advances

RSC Advances

ARTICLE

Synthesis and Characterization of Novel Post-chain Extension Flame Retardant Waterborne Polyurethane

Gang Wu[a], Jinqing Li[a], Chunpeng Chai[a], Zhen Ge[a], Jialun Lin[a], Yunjun Luo[a,†]

A series of novel flame-retardant waterborne polyurethanes with a phosphorus-containing flame retardant diamine (AWPUs) were synthesized by the method of post-chain extension technology and the effect of the chain extender on the properties of AWPU dispersions were investigated. The results revealed that the chain extension increased the molecular weight and the molecular weight distribution. The emulsions stability of AWPUs still kept the stability and particle sizes increased after post-chain extension. AWPUs with post-chain extension of bis (4-aminophenoxy) phenyl phosphine oxide were successfully prepared and characterized by FTIR and NMR analysis. The hydrogen bonds in hard segments and the phase separation between hard segments and soft segments were enhanced. Moreover, the phosphorus-containing chain extender improved the tensile strength but decreased the elongation at break. With the increase of chain extension ratio, the glass transition temperature for hard segments showed an increasing trend but the glass transition temperature for soft segments showed a diverse trend. The phosphorus-containing chain extender reduced the thermal stability of AWPUs and favored the degradation of AWPUs. Finally, the flame retardancy was improved with the flame-retardant extender added.

1 Introduction

Waterborne polyurethanes (WPUs) are non-toxic and tasteless, no pollution to the environment, no danger to the health of operators and cost less, so they have become one of the hotspots of concern.[1-3] However, compared to the solvent-based polyurethane (SPUs), there is still a wide gap for the performance of WPUs especially for their poor mechanical properties, which limit their use in the field of anti-corrosion, waterproof, anti-oxidation and so on.[4] Therefore, many efforts need to do to solve these problems. Generally, the chain extension to WPUs is an effective means to improve the poor properties of waterborne polyurethanes.[5, 6] The low-molecule weight polyols and polyamines are usually used as chain extenders for WPUs, and the chain extension of polyamines could occur during the synthesizing polyurethane prepolymers (internal-chain extension) or after the prepolymer dispersing in water (post-chain extension).[7, 8] Compared with internal-chain extension of polyamines, the post-chain extension consumes fewer organic solvents and it is easy to operate.[9] Some studies have been conducted on the effects of post-chain extension on the properties of WPUs. Li Zhong et al.[10] used different amine such as ethylene diamine (EDA), diethylene triamine (DETA),

and triethylene tetramine (TETA) to chain extend WPU. The results showed after post-chain extension, the thermal and mechanical properties of the modified WPU were significantly improved. Liu Jun et al.[11] prepared a kind of waterborne polyurethanes modified by lignin amines with post-chain extension technology to study the effect of post-chain extension on the aging resistance and mechanical properties. The results showed that the aging resistance and mechanical properties modified WPU were significantly improved with post-chain extension of lignin amines. Kwak et al.[12] studied the effect of different diamines chain extenders on the properties of waterborne polyurethane-urea anionomers. The results showed that particle sizes, thermal degradation temperatures, and mechanical properties of samples increased with the increase of the length of the alkyl chains in diamines.

In the past three decades, flame retardancy has become an important development direction of material modification.[13] The major application fields of WPUs all have a significant demand for flame retardancy. Two approaches can be used to improve the flame retardancy of WPUs: reactive-type flame-retarded method (intrinsic flame-retardant) and blending method.[14] The reactive-type flame-retarded method could overcome shortcomings derived from blending method such as emigration and inhomogeneous mixing, so the reactive-type flame-retarded method could improve the compatibility between flame retardant and WPUs and thus improve the flame retardancy.[15] Therefore, the development of the reactive-type flame-retarded WPUs becomes the direction of

[a.] School of Materials Science and Engineering, Beijing Institute of Technology, Beijing 100081, PR China
† E-mail: yjluo@bit.edu.cn.; Fax: +86 (0)10 68913698; Tel: +86 (0)10 68913698

flame-retardant WPUs studies. Among the reactive-type flame retardants of WPUs, halogen-free phosphorus-containing flame retardants have gradually received wide attention owing to its high flame retardant efficiency, non-toxic and low smoke properties. [16-19] It has also become a very active area in recent researches of flame retardant WPUs. [20-23] Luo Yunjun et al. [24] synthesized a cyclic P-N structure halogen-free phosphorus-containing reactive-type flame retardant: octahydro-2,7-di(N,N-dimethylamino)-1,6,3,8,2,7-di-oxadiazadiphosphecine (ODDP), and introduced it into WPU to prepare flame-retardant WPUs. The results showed that the modified WPU had a good flame retardant property, and the LOI% was up to 30.6 % when loaded 15 wt % ODDP; Chen et al. [25] synthesized two P-N structure reactive-type flame retardant: tri-aziridinyl phosphorus oxide (TAP) and di-aziridinyl-N,N-dimethylaminophosphorus oxide (DDP), and incorporated them into the anionic waterborne polyurethane dispersions to prepare P-N synergist flame-retardant WPUs. It was found that the introduction of phosphorus and nitrogen flame-retardant elements into WPU molecular chains at the same time favored forming a good thermal stability of P-N and C=O bond and a higher char yield, and finally improve the falme retardancy.

However, most studies individually focused on either WPU with post-chain extension or flame-retardant WPU, and little effort was directed toward the effects of flame-retardant post-chain extenders on the properties of WPUs. In this study, we selected a reactive-type phosphorus-containing halogen-free flame retardant diamine - bis (4-aminophenoxy) phenyl phosphine oxide (BPPO) as the flame-retardant post-chain extenders and incorprated it into WPU emulsions to prepare a series of novel flame retardant WPUs by the method of post-chain extension technology. Then several measurements were conducted to study the properties of post-chain extension flame retardant WPUs such as such as particle size and distribution, molecular weight, thermal, mechanical property and flame retardancy. The research was aimed at studying the effects of phosphor-containing diamine and the chain extension ratio on the performance especially flame retardancy of WPUs with post-chain extension.

2 Experimental

2.1 Materials.

Bis (4-aminophenoxy) phenyl phosphine oxide (BPPO) was prepared in our laboratory. [26] Polypropylene glycol (average functionality of 2.0 and Mw of 1000) (PPG1000) was supplied from Tianjin Petrochemical Corporation and dehydrated for 2 h in vacuum at 110°C before use. Toluene diisocyanate (TDI) was supplied by Beijing Xizhong Chemical Plant and used as received. Dimethylol propionic acid (DMPA) was supplied by Beijing Lin refined New Materials Co., Ltd. and heated to 100 °C for 2 h before use. Reagents used in experiments such as acetone, and triethylamine (TEA) were purchased from Sinopharm Chemical Reagent Co., Ltd.

### 2.2 Synthesis of flame-retardant WPUs dispersions with post-chain extension of BPPO.

The synthesis process of flame-retardant WPUs dispersions with post-chain extension of BPPO is shown in Scheme 1. Firstly, a stoichiometric ratio of PPG1000, DMPA and 100 mL acetone were added into a 500 mL three-necked flask equipped with mechanical stirring and the mixture was stirred for 10 min at 60 °C. Then the stoichiometric amount of TDI was slowly dropped. After the adding was completed, the reaction temperature was raised to 85 °C and the reaction continued for about 4 h until the -NCO content was constant. The reaction mixture was then cooled to room temperature and the same mole of TEA with DMPA was added. The neutralization reaction was lasted for 10 min. Afterwards the reaction mixture was added to a certain amount of water to emulsify on a high - speed emulsion machine. The post-chain extension reaction was carried out with BPPO at 25 °C for 30 min. After acetone was distilled off under reduced pressure, a solid content of 40 % of the flame-retardant WPU emulsion was prepared. With this process, a number of different chain extension ratios of post-chain extension flame retardant WPU dispersions were prepared by altering the contents of BPPO.

2.3 Preparation of WPU film.

The obtained aqueous polyurethane dispersions were firstly allowed to stand for 7 days at room temperature in Teflon templates. When water volatilized, the films were placed in a vacuum oven and dried at 80 °C for 24 h, and finally a thickness of about 2 mm transparent polyurethane films were prepared.

2.4 Measurements.

The Fourier transform infrared (FT-IR) spectra of the post-chain extender and WPU films were performed in the range of 4000 - 400cm^{-1} at a 4.0 cm^{-1} resolution over 64 scans using a Thermo FT-IR spectrometer.
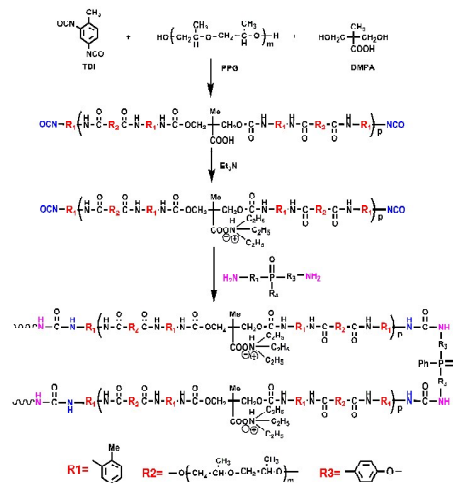
Scheme 1 Synthesis process for WPU dispersions with post-chain extension of BPPO.

A Bruker Spectrospin Advance Series Bruker AV400 NMR spectrometer (Bruker Instruments, Billerica ma) was used to obtain ^{1}H NMR spectra for which DMSO-d_6 were used as solvents.

The mechanical stability was measured on a centrifuge at 4000 r / min for 15 min to see whether there was precipitate or not.

The Zeta potential, the average particle size and distributions of WPU dispersions were measured with a Malvern Nano-ZS laser particle sizer (UK).

The molecular weight of WPU dispersions was measured using a Shimadzu Prominence gel permeation chromatograph (GPC, Japan). All the samples were dissolved in tetrahydrofuran (THF) at a constant concentration 0.1 wt %. The flow rate of THF solvent was 1.0 mL / min and the sample injection volume was 10 μL.

A Mettler Toledo DSC1 differential scanning calorimeter was used to measure the thermal properties of WPU films with the sample weight about 5 - 10 mg, nitrogen atmosphere, heating rate 10 °C / min.

The thermal stability of WPU films were performed on a Mettler-Toledo apparatus with a nitrogen flow of 20 ml /min. Samples (about 5 mg) were heated in Pt pans, from 30 to 600 °C at heating rates of 10 °C /min. The initial decomposition temperature, T_{ini}, at which the sample was start to decomposition, and T_{max}, at which products possessed the maximum weight loss rate, were recorded together with the residue weight.

The Static mechanical tensile stress-strain measurements of WPU films were performed on the Dumbbell-shaped samples using an Instron 1185 testing machine with a cross-head speed of 100 mm / min at room temperature. For each sample, five specimens were tested and the average value is reported.

The Limiting Oxygen Index (LOI) of WPU films was measured using an HC-2 oxygen index meter (Jiang Ning Analysis Instrument Co., China) on 150×50×2 mm^3 sheets according to the standard oxygen index test ASTM D2863-77.

The vertical burning tests (UL-94) of WPU films were conducted by a CZF-II horizontal and vertical burning tester (Jiang Ning Analysis Instrument Co.). The specimens used were 150×50×2 mm^3 according to the UL-94 tests (ASTM D3801-1996 standard).

The cone calorimeter tests (CCTs) were carried out on the cone calorimeter (FTT, US) following the procedures in ISO5660. Square specimens (100×100×2 mm^3) were irradiated at a heat flux of 35 kW /m^2 corresponding to a mild fire scenario.

The XPS spectra were recorded with a VG ESCALAB MK II spectrometer. The X-ray gun was operated at 15 kV voltage and 20mA current. Samples treated at different temperature were measured at room temperature.

3 Results and Discussion

3.1 Molecular weights

Fig.1 showed the changes of molecular weights and PDI of AWPUs with different chain extension ratio of BPPO. Here the chain extension ratio is defined as the percentage of the mole ratio of amino groups of chain extenders to the theoretically

residual NCO groups of WPU dispersions, and the mole of theoretically residual NCO groups is the mole of NCO groups of TDI minus the mole of -OH groups of PPG1000 and DMPA.[10] As seen in Fig.1, the Mn and Mw increased with the increase of chain extension ratio, meanwhile PDI also showed a rising
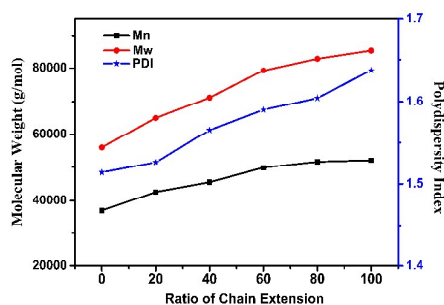

Fig.1 Molecular weights and PDI of AWPUs with different chain extension ratio of BPPO

trend. It could also be found that the molecular weights increased sharply at first until the chain extension ratio of 80 %, and then the increase became less steep. In previous literatures,[27,28] after emulsification the chain extension reaction mainly occurs on the surface of particles, and the reaction between the amino groups and residue NCO groups increased the molecular weight until a specific chain extension ratio. Afterwards because some residue NCO groups may locate in the inside of particles, some NCO groups may be consumed derived from the reaction with water, not all residual NCO functions could react with the chain extenders. It was indicated that there was an actual chain extension ratio which was less than 100 %, and when loaded 100 % of BPPO, some amino groups in chain extender could not react with residual NCO. Therefore, the molecular weights increased quickly before 80 %, and the increase after 80 % resulted from the chain extension with a small amount of NCO functions located in the inside of particles.

3.2 The emulsion stability and particle sizes

Emulsion stability is an important quality specification for
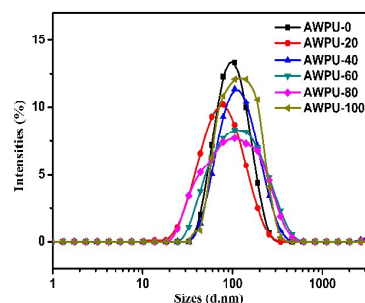
Fig.2 Particle sizes and distributions of AWPU dispersions with different chain extension ratio

RSC Advances

ARTICLE

Table 1 Zeta potential, particle sizes and distributions of AWPU dispersions with different chain extension ratio

Sample	Zeta potential (mV)	particle sizes（d.nm）	PDI	centrifugal stability
AWPU-0	-43.4	91.2	0.133	No precipitate
AWPU-20	-41.4	78.8	0.246	No precipitate
AWPU-40	-40.2	105.8	0.249	No precipitate
AWPU-60	-40.0	114.0	0.249	No precipitate
AWPU-80	-33.6	123.8	0.298	No precipitate
AWPU-100	-30.1	127.5	0.286	Little precipitate

WPUs, and has the significant impact on the storage, transportation and the use of the emulsion. In this work, emulsion stability was measured by mechanical stability tests and Zeta potential tests, and the results were listed in Table 1. After being centrifuged at 4000 r / min for 15 min, as shown in Table 1, all the AWPU emulsions with chain extension ratios from 0 to 80 % showed a stable system with no precipitate, which meant these emulsions exhibited a good mechanical stability, while AWPU with chain extension ratio of 100% had a little precipitate resulted from excess chain extender. Zeta potential can be used to characterize the thickness of hydrated double electric layer of the WPU emulsion particles. For anionic-shape WPUs, Zeta potential are often negative, and the higher its absolute value is, the more thickness of hydrated double electric layer of the WPU emulsion particles and thus the better its mechanical and chemical stability.[29] Therefore, in order to further characterize the emulsion stability of AWPUs with post-chain extension of BPPO, Zeta potential was tested and the results were also shown in Table 1. It could be drawn from Table 1 that the post-chain extension reduced the absolute value of Zeta potential of AWPU. The reason was that the post-chain extension increased the molecule weight and the emulsion particle size. In this article, the amount of DMPA and TEA were identical for each sample. After been fully ionized in water, the total electric charge of each sample was also the same. The larger of the emulsion particles, the less was the charge number per unit area, and the potential difference between the shear plane and the bulk solution (Zeta potential) was decreased.[30] Although the post-chain extension reduced the absolute value of Zeta potential of AWPU, the absolute value of each emulsion was still more than 30 mV. And according to the colloidal stability of the double electrical layer theory: when the absolute value of Zeta potential is greater than 30 mV, the emulsion will have a good stability, therefore, all the AWPU emulsions still kept stable after post-chain extension.

Fig.2 showed the influence of different chain extension ratio on the particle sizes and distributions of AWPU emulsions and the data was listed in Table 1. It was found that the average particle size of AWPU-0 was about 91.2 nm, and the average particle size of AWPU-20 was 78.8 nm. After the chain extension ratios reached 20 %, the average particle sizes showed an increasing trend as the chain extension ratio increased. The decrease of the average particle size for AWPU-20 may be due to the residual NCO reacted with water in the storage stage and resulted in the aggregation of the particles for AWPU-0. As for AWPU-20, there was a small amount of chain extender reacting with the residual NCO which could prevent the aggregation of the particles. Moreover, as shown in Table 1, the size distribution was generally a constantly widening trend except for AWPU-100 resulted from excess chain extender which was accordance with other post- chain extension of WPU studies.[28] In addition, it could also be found that the average particle sizes increased quickly before 80 %, and the increase after 80 % resulted from the chain extension with a small amount of NCO functions located in the inside of particles, which was consistent with the molecular weight.

3.3 Structure of AWPUs

Fig.3 showed the FTIR reflection spectra of AWPUs films with different chain extension ratio of BPPO. As seen in Fig.3, the characteristic peaks at 1736 cm^{-1}, 1610 cm^{-1} and 1100 cm^{-1} were assigned to C=O, -Ph and C-O-C groups, respectively. In addition, the N-H peaks of AWPU films was at about 3300 cm^{-1}, 1518 cm^{-1} and 947 cm^{-1}. The characteristic peaks at 1224 cm^{-1} and 1190 cm^{-1} was respectively assigned to P=O and P-O-Ph, and the intensity increased with the increase of chain extension ratio. In order to further characterize the structure of AWPUs, NMR was introduced. Take AWPU-40 for example. ^{1}H NMR of AWPU-0 and AWPU-40 were shown in Fig.4. As shown in Fig.4, compared to AWPU without BPPO (AWPU-0), there appeared new peaks at 7.8-7.4 ppm for AWPU-40. The new peaks were attributed to the benzene rings derived from the post-chain extension of BPPO. As depicted in Fig.5, there was only one broad peak from 9.5 to 9.1 in the ^{31}P NMR spectrum, while the peak of pure BPPO was at about 13.2 ppm in the ^{31}P NMR spectrum.[31, 32] The results above indicated that BPPO was bonded to the waterborne polyurethane molecules.
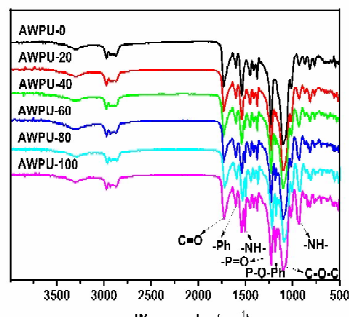
Fig. 3 FTIR curves of flame-retardant WPUs films with different chain extension ratios
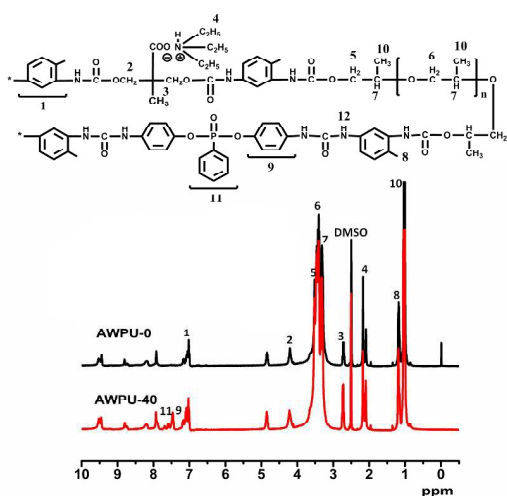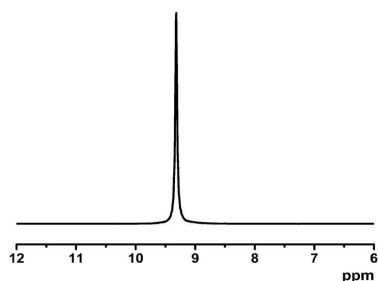

Fig. 4 ^{1}H NMR of AWPU-0 and AWPU-40.

Fig. 5 ^{31}P NMR of AWPU-40.

3.4 Hydrogen bonding analysis

As well known, WPUs present excellent thermal and mechanical performances due to the micro-phase separation caused by the

thermodynamic incompatibility between the hard and soft segments, and the degree of micro-phase separation of WPU is closely related to the presence of hydrogen bonds.[33]

Among the hydrogen bonding in WPUs, hydrogen bonding between the N-H group (hard segment: HS) and C=O groups in urethane and urea (HS) is responsible for the phase separation, while hydrogen bonding between the N-H group (HS) and ether linkages (soft segment: SS) favors the phase mixing.[34] In order to study the hydrogen bonding of AWPUs with different chain extension ratio, FTIR was used as an effective method. In this work, FTIR of N-H and C=O regions was used to study the hydrogen bonding of AWPUs.[35-37] For complex peaks such as N-H and C=O regions, curve-fitting simulations were performed using curve-fitting functions on Origin software 8.0. The v (N-H) and v (C=O) bands were deconvoluted using Gaussian curve-fitting simulations to get the best fit Gaussian peaks. For deconvolution study, the second derivatives of spectra in v (C=O) and v (N-H) zones was used to find out the number of Gaussian peaks, and the deconvolution process was conducted on the omnic software to determine the peak position and the peak width. Before deconvolution, a flat baseline was chosen in between 3800 and 3000 cm^{-1} for v (N-H) bands and between 1800 and 1600 cm^{-1} for v (C=O) bands and the spectra was corrected by subtracting the baseline.

Fig.6 was the FTIR spectra of C=O regions in AWPUs with different chain extension ratio and the representative deconvolution of C=O zones in AWPU-100. As shown in Fig.6 (a), the characteristic peaks of C=O regions showed a decrease trend for forming stronger hydrogen bonding with the increase of chain extension ratio, which meant the increasing of the hydrogen bonds. That's because the hydrogen bonding changes the bonding force constant as well as the bond order, and results in the characteristic peaks shifting to a lower stretching vibration frequency.[34, 38] During the multi-peaks fitting simulations, C=O band could be deconvoluted to four peaks and all the fitting correlation were more than 0.999. Here AWPU-100 was selected as the representative, as shown in Fig.6 (b), the C=O peak of AWPU-100 was divided into four peaks respectively corresponding to the free C=O from urethane groups (1733 cm^{-1}), free C=O from urea groups (1703 cm^{-1}), bonded C=O from urethane groups (1678 cm^{-1}), and bonded C=O from urea groups (1652 cm^{-1}).[39] All the results of multi - peaks fitting of AWPU system were listed in Table 2. As seen in Table 2, the percent of hydrogen bonded carbonyls from urea zone in total hydrogen bonded carbonyls (X_{AH}) increased as more post-chain extender added, however, the percent of hydrogen bonded carbonyls from urethane zone in total hydrogen bonded carbonyls (X_{UH}) presented an diverse trend. The reason is that the chain extension of BPPO increases the amount of urea bonds, and since the polarity of urea bonds are bigger compared with urethane bonds, therefore, the hydrogen bonded carbonyls from urea zone the polarity of urea bonds are bigger compared with urethane bonds, therefore, the hydrogen bonded carbonyls from urea zone increased with the increase of chain extension ratio[34]. These results indicated that post-chain extension with high polarity BPPO could selectively enhance the intermolecular

force in hard segments and favor the phase separation between the hard segments and soft segments.[40]

Fig.7 was the FTIR spectra of N-H zone with different chain extension ratio and the representative FTIR peaks of deconvolution of N-H zones in AWPU-100, and the results of FTIR peaks of deconvolution were listed in Table 3. Among the AWPUs, N-H band could also be deconvoluted to four peaks and all the correlation coefficients of the fitting process were more than 0.995. Take AWPU-100 as the representative, as shown in Fig.7 (b), the bands at 3491, 3408, 3304 and 3196 cm^{-1} were respectively corresponding to free N-H groups, N-H

groups bonded with C=O groups or P=O in hard segments (responsible for the phase separation), N-H groups bonded with ether oxygen in soft segments (favoring the phase mixing) and an overtone of deformation vibration of N-H group from Fermi resonance.[34, 41, 42] In addition, as shown in Table 3, the
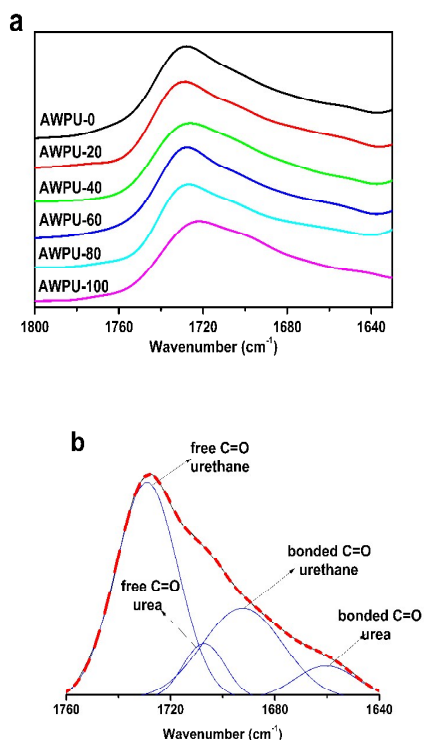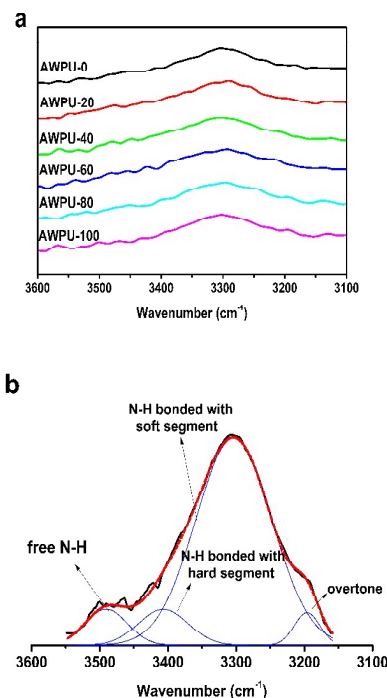
Fig.7 FTIR spectra of N-H regions in AWPUs with different chain extension ratios (a) and FTIR peaks of deconvolution of N-H zones in AWPU-100 (b)

Fig.6 FTIR spectra of C=O regions in AWPUs with different chain extension ratios (a) and FTIR peaks of deconvolution of C=O zones in AWPU-100 (b)

Table 2 FT-IR analysis result of carbonyl group

| Sample | urethane | | | | urea | | | | X_H (%) | X_{UH} (%) | X_{AH} (%) |
| | free | | bonded | | Free | | bonded | | | | |
	ν /cm^{-1}	area	ν /cm^{-1}	area	ν / cm^{-1}	Area	ν /cm^{-1}	area			
AWPU-0	1733	2.20	1680	0.32	1706	0.79	1657	0.17	14.0	65.3	34.7
AWPU-20	1732	1.76	1679	0.24	1701	0.62	1656	0.15	14.1	61.5	38.5
AWPU-40	1732	2.05	1678	0.35	1703	0.69	1656	0.26	15.4	57.4	42.6
AWPU-60	1733	1.11	1678	0.15	1705	0.35	1655	0.14	16.6	51.7	48.3
AWPU-80	1734	1.01	1677	0.11	1703	0.29	1653	0.17	17.7	39.3	60.7
AWPU-100	1733	2.59	1677	0.37	1703	0.64	1652	0.59	22.9	38.5	61.5

X_H is percent of total hydrogen bonded carbonyls; X_{UH} is percent of hydrogen bonded carbonyls from urethane in total hydrogen bonded carbonyls; X_{AH} is percent of hydrogen bonded carbonyls from urea regions in total hydrogen bonded carbonyls.

RSC Advances

ARTICLE

Table 3 FT-IR analysis result of N-H group

Sample	free		bonded in HS		bonded in SS		overtone		X_f / %	SS/HS
	v/cm^{-1}	area	v/cm^{-1}	area	v/cm^{-1}	area	v/cm^{-1}	area		
AWPU-0	3479	0.29	3415	0.04	3297	0.56	3190	0.03	31.5	14
AWPU-20	3480	0.18	3408	0.03	3299	0.39	3217	0.06	27.4	13
AWPU-40	3482	0.11	3393	0.04	3300	0.48	3204	0.02	16.9	12
AWPU-60	3483	0.11	3392	0.05	3300	0.56	3199	0.03	15.0	10.4
AWPU-80	3483	0.11	3385	0.07	3302	0.67	3198	0.02	12.2	9.3
AWPU-100	3491	0.05	3370	0.06	3304	0.53	3196	0.03	7.4	8.8

content of free N-H decreased with the increase of BPPO, which meant that the total hydrogen bonds in AWPUs were increasing with BPPO added. Furthermore, compared the deconvoluted peaks at 3408 and 3304 cm^{-1} in AWPU-100 as shown in Fig.7 (b) and Table 3, it could be drawn that the ratio of the areas of phase mixing to that of phase separation was decreased with the increase of chain extension ratio, although the area of phase mixing was higher than that of phase separation. It is indicated that the phase separation increased with post-chain extension of BPPO resulted from forming stronger hydrogen bonds in hard segments.

3.5 Mechanical properties

Mechanical properties measurement is an important test for AWPUs, that's because mechanical performance directly affects the application of the materials. Fig.8 was the results of mechanical tests for AWPUs with different chain extension of BPPO. It could be drawn from Fig.8 that adding BPPO improved the strength of WPUs, but reduced the toughness of WPUs, and the more BPPO added, the more of the increase or the decrease. Furthermore, compared to AWPU-0, the tensile strength for AWPU-100 increased by 37%, while the elongation at break for AWPU-100 decreased by 31 %. The reason is that the high polar diamine - structure BPPO was conductive to form more hydrogen bonds in hard segments and promote forming stronger hard segment inter-chain cohesive force after post-chain extension. The hydrogen bonding between the hard segments was attributed to form paracrystalline or crystalline structure in hard segments phase, thus finally increased the tensile strength. Furthermore, the high polar post-chain extender promoted more hard segments to enter into the soft segments and contributed to increase the number of physical crosslinking, thus reduced the content of the flexible chains, and therefore the elongation at break was decreased with the increase of chain extension ratio of BPPO.

3.6 Thermal properties
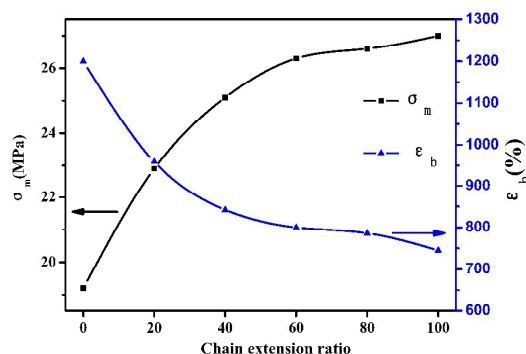
Fig.8 The strength and elongation at break for flame-retardant WPU with different chain extension ratio of BPPO

The thermal properties of AWPUs with various chain extension ratios of BPPO were studied by differential scanning calorimetry (DSC). Fig.9 and Table 4 were DSC curves and DSC data for flame retardant AWPUs with various chain extension ratios. Fig.9 showed that all the AWPUs samples had two glass transition temperature T_gs and T_gh, respectively corresponding to glass transition temperature of soft segments and hard segments in AWPUs molecules. The results indicated that the WPUs had apparent micro-phase separation. Moreover, T_gh gradually increased with BPPO added, whereas T_gs showed a diverse trend. Because the difference of two temperatures, ΔT_g (T_gh -T_gs), is related with the extent of microphase separation between soft and hard segments in polyurethane, and the value of ΔT_g is bigger, the micro-phase separation is more serious. So the bulk phase separation increased in BPPO containing chain extender, which was accordance with FTIR
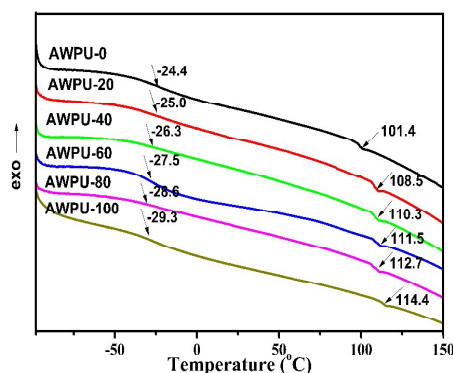
Fig.9 DSC of AWPUs with different chain extension ratios

Table 4 DSC data for flame retardant WPU with various chain extension ratios of BPPO

sample	T_g (°C)		
	T_gs	T_gh	ΔT
AWPU-0	-24.4	101.4	125.8
AWPU-20	-25.0	108.5	133.5
AWPU-40	-26.3	110.3	136.6
AWPU-60	-27.5	111.5	139.0
AWPU-80	-28.6	112.7	141.3
AWPU-100	-29.3	114.4	143.7

results that the high polar diamine-structure extender resulted in a better phase separation. In addition, as drawn from the deconvoluted FTIR spectra, BPPO selectively enhanced the hard segment cohesion and reduced the inter-molecular forces between the hard segments and soft segments and therefore the T_gh was increased while T_gs was decreased after chain extension of BPPO.

3.7 Thermal stability properties

Fig.10 was TGA (a) and DTGA (b) curves of flame retardant AWPUs with various chain extension ratios in N_2, the results was listed in Table 5. We learned from Fig.10 that there were two main stages of degradation for AWPU without post-chain extension of BPPO (AWPU-0) resulted from urethane and urea groups in hard segment and polyether soft segment, respectively.[43] However, compared with AWPU-0, there were three main stages of degradation for AWPUs with post-chain extension of BPPO respectively corresponding to the degradation of phosphate groups in BPPO molecules, urethane and urea groups in hard segment and polyether soft segment. However, although there were three stages of degradation for AWPUs, the distinction between the first two stages of degradation was not obvious. Moreover, the weight loss for all AWPUs at 204 °C was responsible for the degradation of low-molecular weight polyols and DMPA.

For AWPU-0, as shown in Table 5, its T_{ini} was 191.2 °C and two temperatures at the maximum degradation rate were 282.7 °C for the degradation of urethane and urea groups and 391.2 °C for the degradation of polyether chains, furthermore, AWPU-0

only had a small amount of char residue of 1.4 % at 600 °C under N_2 atmosphere. With unexpected, the AWPU with the addition of BPPO reduced T_{ini} and it seems that the larger the addition amount was, the lower the T_{ini} value would be (seen in Table 5). The results above observed could be attributed to that BPPO has a lower initial decomposition temperature than AWPU-0. Concerning AWPUs with post-chain extension of BPPO, the temperatures at which three maximum weight losses occurred (T_{max1}, T_{max2} and T_{max3}) for AWPUs with different chain extension ratios of BPPO showed a similar trend that T_{max1} and T_{max3} were gradually decreased, and the more chain extender added, the sooner of the complete decomposition of AWPUs. The results above indicated that phosphorus-containing chain extender reduced the thermal stability AWPU and accelerated the degradation of waterborne polyurethane molecule chains. Moreover, in contrast with AWPU-0, the post-chain extension increased T_{max2} due to forming strong intermolecular forces and high polar urea groups. Besides of the changes of the temperature, the amount of the char residues increased with the increase of chain extension ratios of BPPO, for instance, AWPU-100 had a char residue of 5.6 % compared with 1.4 % of AWPU-0. The more char residues indicated BPPO had the condensed phase flame retardant effect. The more char residues acted as a barrier and helped to inhibit gaseous products from diffusing to the flame and to shield the polymer surface from heat and oxygen, consequently, improved the flame retardancy of AWPU with post-chain extension of BPPO.
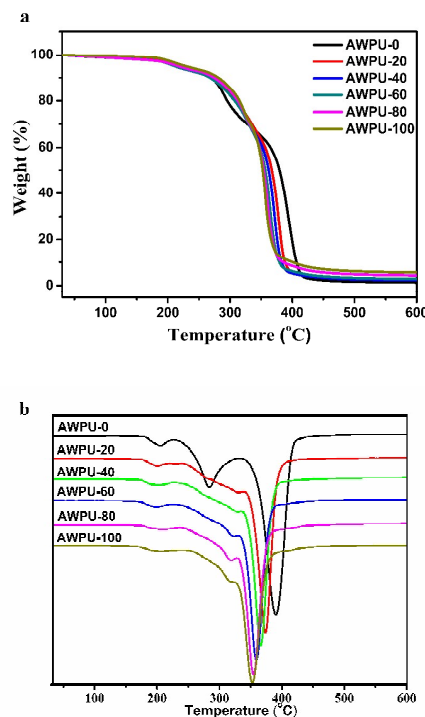

Fig.10 TGA (a) and DTGA (b) curves of AWPUs with different chain extension ratios

Table 5 Thermo stability Data of AWPUs with different chain extension ratios of BPPO

sample	T_{ini}	T_{max} (^{o}C)			residues at 600 (^{o}C) (%)
		first step	second step	third step	
AWPU-0	245.3	-	282.7	391.2	1.4
AWPU-20	245.1	281.0	327.2	374.8	2.3
AWPU-40	244.8	280.4	325.9	367.4	2.5
AWPU-60	244.6	280.4	321.3	360.0	2.9
AWPU-80	244.4	280.2	318.4	353.9	4.4
AWPU-100	244.4	279.6	316.9	352.5	5.6

Table 6 LOI% and UL-94 data for flame-retardant AWPU with different chain extension ratio of BPPO.

| Sample	P (wt %)	N (wt %)	LOI %	UL-94
AWPU-0	0	0	24.1	No rating
AWPU-20	0.27	0.24	26.4	No rating
AWPU-40	0.52	0.47	27.7	V-2
AWPU-60	0.76	0.68	28.2	V-2
AWPU-80	0.98	0.89	29.2	V-1
AWPU-100	1.19	1.07	30.1	V-0

3.8 Fire properties

The results of LOI and UL-94 tests for AWPUs with post-chain extension of BPP were listed in Table 6. As seen from Table 6, for AWPU-0 the LOI value was 24.1%, and UL-94 test showed no rating and forming much molten-dripping when burning. However, when more BPPO was added, the LOI values rose shapely. When loaded 100 wt% of BPPO, the LOI value reached 30.1 %, and UL-94 got a rating of V-0, meaning that BPPO had excellent flame retardancy. According to the results from TGA, BPPO could attribute to form more residue char and serve as the condensed phase flame-retardant effect, and with more BPPO added, the flame retardancy was improved.

Because of the requirement for small sample size and low heat input, LOI tests and UL-94 tests are widely used in evaluating flame retardancy of the flame retardants.[44] However, for a real scale fire, the LOI values and UL-94 results are not reliable. Fortunately, cone calorimetric tests could simulate the real scale fire and could be considered to be an effective test method.[45] With cone calorimeters tests, various parameters including the time to ignition (t_{ign}), the peak heat release rate (PHRR), the total heat release (THR), average mass loss rate (AMLS), and average-specific extinction area (ASEA), a measure of the amount of smoke evolved could be obtained,[46] among which the most important parameters were PHRR and THR.

Fig.11 and Table 7 presented the fire performance and the detailed data. As seen in Fig.11, after ignition, AWPU-0 burned quickly and evolved a large amount of heat with a PHRR of 1134 kW / m^2. When chain extended by BPPO, as shown in Fig.11, t_{ign} showed an increasing trend and the burning was delayed compared with AWPU-0. In addition, both PHRR and the THR were considerably reduced with the incorporation of

BPPO, for example, the PHRR and the THR were reduced by 57.1 % and 41.6 %, respectively. Table 7 showed various parameters with different chain extension ratios giving a lot of information. Table 7 showed a similar trend that parameters like PHRR, AHRR, THR and AMLR were decreased with the increase of chain extension ratio. Of these parameters in cone calorimeters data, ASEA was associated with smoke and gas released, and can be used to explain gas phase flame retardant mechanism for flame retardant materials.[47] From Table 7, ASEA of AWPUs with post-chain extension of BPPO showed a signicantly increasing trend with respect to AWPU-0, which meant WPUs with post-chain extension of BPPO may have excellent gas phase flame retardant effect. The fire performance index (FPI) was usually selected to judge the fire hazard because there is a certain correlation between the value of FPI of materials and the fire risk. It is generally accepted that the bigger the value of FPI of a material is and the lower its fire risk will be, and vice versa. The FPI is defined as the proportion of t_{ign} and the peak HRR.[48] From Table 6, it can be seen that FPI is increasing with more BPPO added indicating the fire risk of WPUs with post-chain extension of BPPO is decreased. It may be reasonable to draw a conclusion that the changes of these parameters might indicate WPUs with post-chain extension of BPPO have excellent flame retardancy and BPPO was an excellent flame retardant.
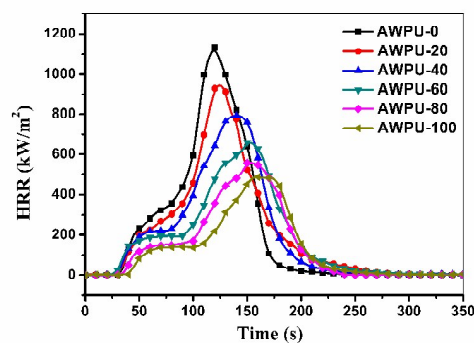

Fig.11 Heat release rate (HRR) curves for flame retardant WPU with various chain extension ratios at 35 kW / m^2

RSC Advances

ARTICLE

Table 7 Cone calorimeters data for flame retardant WPU with various BPPO loading (%) at 35kW / m^2

sample	t_{ign}	PHRR (kW/m^2)	AHRR (kW/m^2)	THR (MJ/m^2)	AMLR (g/s)	ASEA (m^2/kg)	FPI (m^2s/KW)
AWPU-0	25	1134	280	76	0.066	182	0.022
AWPU-20	26	953	248	72	0.062	373	0.027
AWPU-40	28	792	218	67	0.049	404	0.035
AWPU-60	30	661	174	61	0.042	415	0.045
AWPU-80	35	559	135	50	0.037	435	0.063
WPU-100	39	486	108	44	0.035	450	0.080
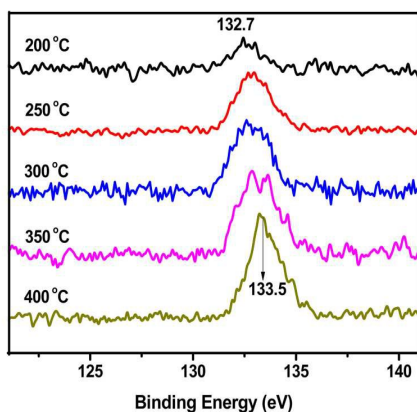
Fig.12 P_{2p} XPS spectra of AWPU-100 treated at various temperatures.

XPS was a good method to study the flame retardant mechanism. The P_{2p} XPS spectra of the heat-treated AWPU-100 samples are shown in Fig.12. As shown in Fig.12, the main peak shifts upward from 132.7 eV at 200 ^{o}C to 133.5 eV at 400 ^{o}C. The binding energy in the range of 132.7 to 133.5 eV has been assigned to PO^{3-} groups,[49] which forms during the thermal degradation of phosphorus-containing compounds. In previous literature,[50, 51] the phosphorous-containing flame-retardants have excellent flame retardancy due to the condensed phase flame retardant effect of phosphoric acid or polyphosphoric acid derived from the degradation of the phosphorous-containing flame-retardants. Therefore, BPPO increased the flame retardancy of AWPUs when burning.

4 Conclusions

In this work, a series of post-chain extension flame retardant AWPUs were prepared by the method of post-chain extension technology and the influences of chain extension ratio on the properties of WPU dispersions were investigated. The results showed that the molecular weights of AWPUs increased with the increase of chain extension ratio; the post-chain extension increased the particle sizes of WPU dispersions but still kept the stability; the hydrogen bonds in hard segments and the phase separation between hard segments and soft segments were enhanced with post-chain extension reaction; the tensile strength was improved but the elongation at break was decreased as BPPO added; T_gh increased but T_gs decreased with post-chain extension of BPPO; BPPO reduced the thermal stability of AWPUs and promoted the degradation process; and finally the flame retardancy of AWPUs was improved with the increase of BPPO. Those results showed that the post-chain extension had an important influence on the properties of AWPUs, and BPPO was thought to be an effective chain extender with high flame retardancy that improved the properties of AWPUs.

Notes and references

1. Lu Y, Larock RC, Biomacromolecules, 2008, 9:3332-3340.
2. Cao X, Chang PR, Huneault MA, Carbohydr Polym., 2008, 71:119-125.
3. McCabe RW, Taylor A, Green Chem, 2004, 6:151-155.
4. Lefebvre, J.Bastin, B.Bras, M.L.Duquesne, S.Ritter, C.Paleja, R.Poutch, F, Polym. Test., 2004, 23:281-290.
5. Ajaya K. Nanda, Douglas A. Wicks, Samy A. Madbouly and Joshua U. Otaigbe, Journal of Applied Polymer Science, 2005, 98(6): 2514–2520.
6. Marcia C Delpecha and Fernanda M.B Coutinho, Polymer Testing, Polymer Testing, 2 000, 19(8):939-952.
7. P. Florian, K.K. Jena, S. Allauddin, R. Narayan, K. Raju, Ind. Eng. Chem. Res., 2010, 49: 4517–4527.
8. Y. Wang, C. Ruan, J. Sun, M. Zhang, Y. Wu, K. Peng, Polym. Degrad. Stabil., 2011, 96: 1687–1694.
9. Y. Nomura, A. Sato, S. Sato, H. Mori, T. Endo, J. Polym. Sci., Part A: Polym. Chem, 2007, 45: 2689–2704.
10. Liang Lei, Li Zhong, et al., Chemical Engineering Journal, 2014, 253: 518-525.
11. Jun Liu, Hai-Feng Liu, Qing-Xiang Guo, et al., Journal of Applied Polymer Science, 2013, 130 (3): 1736-1742.

12. Y.S. Kwak, S.W. Park, H.D. Kim, Colloid Polym. Sci., 2003, 281: 957-963.
13. Song, Y. P.; Wang, D. Y.; Wang, X. L.; Lin, L.; Wang, Y. Z, Polym. Adv. Technol., 2011, 22, 2295-2301.
14. Neisius, M.; Liang, S.; Mispreuve, H.; Gaan, S, Ind. Eng. Chem. Res., 2013, 52(29):9752-9762.
15. Ranganathan, T.; Zilberman, J.; Farris, R. J.; Coughlin, E. B.; Emrick, T, Macromolecules. 2006, 39, 5974-5975.
16. Perez R M, Sandler J K W, Altstadt V, Hoffmann T, Pospiech D, Journal of Applied Polymer Science, 2007, 105(5):2744-2759.
17. Youssef B, Mortaigne B, Soulard M, Saiter J.M, Journal of Thermal Analysis and Calorimetry, 2007, 90(2):489-494.
18. Ranganathan T, Ku B C, Zilberman J, Beaulieu M, Farris R J, Coughlin E B, Emrick T, Journal of Polymer Science Part A: Polymer Chemistry, 2007, 45(20):4573-4580.
19. Tao K, Li J, Xu L, et al., Polymer Degradation and Stability, 2011, 96(7): 1248-1254.
20. Zhu S W, Shi W F, Polymer International, 2004, 53:266-271.
21. Youssef B, Lecampe L, Khatib W E, Bunel C, Mortaigne B, Macromolecular Chemistry and Physics, 2003, 204 (15):1842 -1850.
22. Gao F, Tong L F, Fang Z P, Polymer Degradation and Stability, 2006, 91(6): 1295-1299.
23. Finocchiaro P, Consiglio G A, Imbrogiano A, Failla S, Phosphorus Sulfur and Silicon and the Related Elements, 2007, 182(8): 1689-1701.
24. Limin Gu, Zhen Ge, Muhua Huang, Yunjun Luo, Journal of Applied polymer Science，2015, 132(3): 41288.
25. C H Shao, J J Huang, G N Chen, et al, Polymer Degradation and Stability, 1999, 65: 359-371.
26. Liu, Y. L.; Hsiue, G. H.; Lan, C. W.; Chiu, Y. S., J Polym Sci Part A: Polym Chem, 1997, 35, 1769.
27. Y.K. Jhon et al, Colloids and Surfaces A: Physicochem. Eng. Aspects, 2001, 179:71–78.
28. J. Yoon Jang, Y. Kuk Jhon, I. Woo Cheong, J. Hyun Kim, Colloids Surf. A Physicochem. Eng. Aspects, 2002, 196:135-143.
29. Kim B K, Colloid and Polymer Science, 1996, 274(7): 599-611.
30. Hang Li, Shiqiang Wei, Changle Qing, and Jinshan Yang, Journal of Colloid and Interface Science, 2003, 258:40-44.
31. Zhu S W, Shi W F., Polymer International, 2004, 53:266-271.
32. Youssef B, Lecampe L, Khatib W E, Bunel C, Mortaigne B, Macromolecular Chemistry and Physics, 2003, 204 (15):1842 -1850.
33. J.Macknight and M.Yang. J.Polym.Sci, : Symp., 1973,42:883.
34. Aswini K. Mishra, D.K. Chattopadhyay, B. Sreedhar and K.V.S.N. Raju, Progress in Organic Coatings, 2006, 55:231–243.
35. Ubale, V. P.; Sagar, A. D.; Birajdar, M. V, J. Appl. Polym. Sci., 2001, 79(3), 566-571.
36. Kaushiva, B. D.; Wilkes, G. L, Polymer, 2000, 41(1), 285-310.
37. Schuur, M. ver der.; Noordover, B.; Gaymans, R. J., Polymer, 2006, 47, 1091-1100.
38. D.F. Varnell, J.P. Runt, M.M. Coleman, Macromolecules, 1981, 14:1350-1356.
39. Teo, L. S.; Chen, C. Y.; Kuo, J. F, Macromolecules, 1997, 30, 1793-1799.
40. D.P. Queiroz, M.N. De Pinho, C. Dias, Macromolecules, 2003, 36:4195-4200.

41. V. Romanova, V. Begishev, V. Karmanov, A. Kondyurin, M.F. Maitz, J. Raman Spectrosc, 2002, 33(10):769-777.
42. Pion Florian, Kishore K. Jena, Shaik Allauddin, Ramanuj Narayan, and K. V. S. N. Raju, Ind. Eng. Chem. Res., 2010, 49, 4517–4527.
43. S.Levchik, E.D.Weil, Polym. Int., 2004, 53(11):1585-1610.
44. S.Y. Lu and I. Hamerton, Prog. Polym. Sci., 2002, 27, 1661-1712.
45. B. Scharte, M. Bartholmai, and U. Knoll, Polymer Degradation and Stability, 2005, 88(3):540-547.
46. G. Gillina, E. Bravin, C. Badalucco, G. Audisio, M. Armannini, A.D. Chirico, and F. Provasoli, Fire Materials, 1998, 22, 15-18.
47. Guobo Huang, Jianrong Gao, Yujing Li, Liang Han, Xu Wang, Polymer Degradation and Stability, 2010, 95(2):245-253.
48. Shoulin Fang, Yuan Hu, Lei Song, Jing Zhan, Qingliang He, Journal of Materials Science, 2008, 43(3):1057-1062.
49. Shengwu Zhu, Wenfang Shi, Polymer Degradation and Stability, 2003, 80: 217-222.
50. Jansen RJJ, Vanekkum HV, Carbon, 1995, 33: 1021-1027.
51. Limin Gu, Yunjun Luo, Ind. Eng. Chem. Res., 2015, 54, 2431-2438.
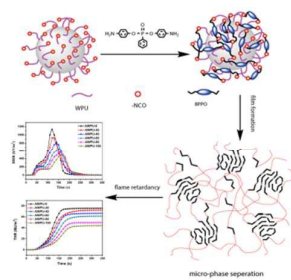
RSC Advances Accepted Manuscript

Flame-retardant waterborne polyurethanes with a phosphorus-containing flame retardant diamine (AWPUs) were synthesized and characterized by the method of post-chain extension technology.